

Numerical Simulation of Electroosmotic Flow with Step Change in Zeta Potential

X. Chen¹, Y.C. Lam^{1,2}, X.Y. Chen², J.C. Chai² and C. Yang²

¹Singapore-MIT Alliance Programme, Nanyang Technological University, Singapore 639798

²School of Mechanical & Production Engineering, Nanyang Technological University, Singapore 639798.

Abstract— Electroosmotic flow is a convenient mechanism for transporting polar fluid in a microfluidic device. The flow is generated through the application of an external electric field that acts on the free charges that exists in a thin Debye layer at the channel walls. The charge on the wall is due to the chemistry of the solid-fluid interface, and it can vary along the channel, e.g. due to modification of the wall. This investigation focuses on the simulation of the electroosmotic flow (EOF) in a cylindrical microchannel with step change in zeta potential. The modified Navier-Stoke equation governing the velocity field and a non-linear two-dimensional Poisson-Boltzmann equation governing the electrical double-layer (EDL) field distribution are solved numerically using finite control-volume method. Continuities of flow rate and electric current are enforced resulting in a non-uniform electrical field and pressure gradient distribution along the channel. The resulting parabolic velocity distribution at the junction of the step change in zeta potential, which is more typical of a pressure-driven velocity flow profile, is obtained.

Keywords— Electroosmotic flow, Electrical double-layer, Pressure-driven flow, Zeta potential.

I. INTRODUCTION

Interests in fluid flow in microfluidic devices have received significant attention over the past decade by its potential applications in analytical and bioanalytical chemistry [1-2]. Examples of fluid manipulations include

Manuscript received November 19, 2004.

X. Chen & X.Y. Chen are Research Fellows of the SMA's IMST programme at Nanyang Technological University (E-mail: mxchen@ntu.edu.sg; xychen@ntu.edu.sg respectively).

Y. C. Lam is a SMA (Singapore-MIT Alliance) Fellow at IMST (Innovation in Manufacturing Systems & Technology) Programme. He is also a Professor of the School of Mechanical and Production Engineering, Nanyang Technological University; (Corresponding author; Y.C. Lam; E-mail: yclam@ntu.edu.sg Phone: +65-67905866; Fax: +65-68627215).

J.C. Chai & C. Yang, are Associate Professor and Assistant Professor respectively of the School of Mechanical and Production Engineering, Nanyang Technological University (Email: mckchai@ntu.edu.sg; mcyang@ntu.edu.sg respectively)

dynamic cell separations [3-4], surface patterning of cells and proteins [5], mass spectrometer delivery modules [6] and mixing of two different analytes. Flows driven by an external electric field based on electroosmosis [8] and applied pressure gradient [9] are two methods commonly used for continuous flow in microchannel devices. Electroosmotic flow has wide applications as it has a uniform flow velocity profile and no moving parts [10].

The driving force for electroosmotic flow in microchannels depends on the local net-charge density and strength of the externally applied electrical field. The net-charge density is dependent on the EDL field and hence on zeta potential. Generally, zeta potential is a function of the ionic valence, the ionic concentration of the electrolyte solution, and the surface properties of the microchannel wall. For a system with a simple electrolyte solution and a homogenous channel wall, zeta potential is considered constant. However, the charge on the wall is a function of the chemistry of the solid-fluid interface and can vary along the channel either by design or surface modification, which can cause different zeta potential distribution. As such, in a first step to understand the flow behaviour in such a situation, we model the flow behaviour where there is a step change in zeta potential.

Yang et. al. [11-12] considered pressure-driven flow in a rectangular microchannel. A two-dimensional electric potential model was proposed, and was solved both analytically using the Debye-Huckel linear approximation and numerically. A Green's function approach was developed to obtain a close-form solution of the flow field [11]. They studied the microchannel flow in the fully developed region and avoided the entry region effects and pressure gradient term in the modified Navier-Stokes equations. Patankar et. al. [13] employed a similar model to investigate 3D microchannel flow.

Several researchers [14-18] have studied the effects of variable zeta potential on electroosmotic flow. Anderson et. al. [14] developed an infinite-series solution for flow in a cylindrical microchannel with a zeta potential varying as a cosine or sine function in the flow direction. Potocek et. al. [15] studied the influence of the discrete step change in zeta potential on the velocity profile of the electroosmotic

flow by considering the zeta potential change between two steps. Long et. al. [16] considered a similar type of zeta potential variation in planar and cylindrical capillaries and developed approximations by considering the heterogeneity as small perturbations to the velocity. Stroock et. al. [17] studied two types of surface-charge variation along a direction perpendicular to the applied electrical field, which generates a two-directional electroosmotic flow. By having surface-charge variation along a direction parallel to the electrical field, a recirculating flow is generated. Herr et. al. [18] experimentally investigated the electroosmotic flow field and the sample dispersion rate in open capillaries with a step change in zeta potential and presented a simple model for the fluid velocity and the dispersion rate. The thin EDL assumption is valid only for systems with high ionic concentrations. The above-mentioned investigation all assumed thin electrical double layer and, hence, did not completely consider the effects of EDL field. It is known that the electrical body force responsible for electroosmotic flow depends on the local net-charge density. Therefore, a more general treatment to the effects of zeta potential or EDL variation on electroosmotic flow should consider the change of local net-charge density along the channel. This requires solving for the Poisson-Boltzmann equation, which governs the EDL field. Li et. al. [19-20] and Yang et. al [21-22] studied the variation of the EDL field and step change of zeta potential on the velocity field by adopting the Nernst-Planck equations. However, their works did not consider completely the continuity of electrical current.

In this study, we investigated numerically electroosmotic flow in a cylindrical microchannel with step change in Zeta potential. The modified Navier-Stoke equation governing the velocity field and a non-linear two-dimensional Poisson-Boltzmann equation governing the electrical double-layer (EDL) field distribution. In the junction region of the step change in zeta potential, the changes in parameters are solved numerically by using finite control-volume method. Unlike other models, the continuities of both flow rate and electric current were enforced.

II. MATHEMATICAL FORMULATIONS

A. Governing equations

Figure 1 shows a cylindrical microchannel of radius a and length l and a Cartesian coordinate system for the analysis of the electroosmotic flow. The liquid in the microchannel is assumed to be an incompressible, Newtonian, symmetric electrolyte (1:1) of constant density ρ and viscosity μ . To consider EDL and

electrostatic field effects on fluid flow through the microchannel, the distribution of electrical potential and net charge density in the cylindrical microchannel must be evaluated. Our mathematical model is based on the Navier-Stokes equation, including a term for electrokinetic effect. There are three sets of equations to be solved simultaneously

a). Electrical Field

The step change in zeta potential was considered for a cylindrical microchannel, as shown in Figure 1. For

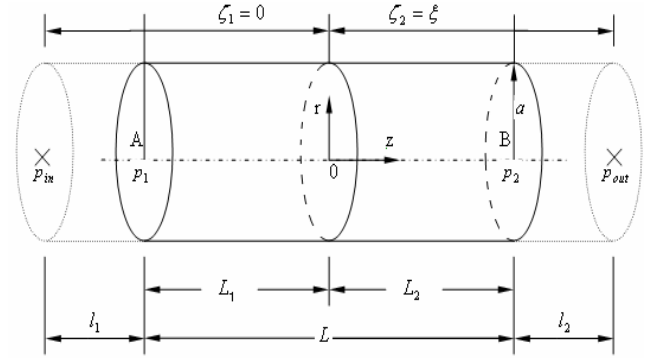


Figure 1 A cylindrical microchannel with a step change in zeta potential.

simplicity, we neglected the differences in permittivity and considered only the deviations of electric field strength. According to the theory of electrostatic, the EDL potential in the cylindrical microchannel is governed by the two-dimensional Poisson equation, given as:

$$\frac{\partial}{\partial z} \left(\epsilon_r \frac{\partial \psi}{\partial z} \right) + \frac{1}{r} \frac{\partial}{\partial r} \left(r \epsilon_r \frac{\partial \psi}{\partial r} \right) = -\frac{\mathbf{r}_e}{\epsilon_o} \quad (1)$$

where ϵ_r is the dielectric constant of the electrolyte, ψ is the electrostatic potential, and ϵ_o is the permittivity of vacuum. The axial and radial coordinates are z and r , respectively. The total net electric charge, \mathbf{r}_e is given by

$$\mathbf{r}_e = e(Z_+ n_+ + Z_- n_-) \quad (2)$$

where e is the elementary charge and Z_+ and Z_- are valences of the co-ions and counter-ions, respectively. n_+ and n_- are the co-ion and counter-ion number concentrations respectively. In thermodynamics equilibrium where the chemical potential is balanced by the electrical potential, it can be shown that both n_+ and n_- follow the Boltzmann distributions [23]:

$$n_+ = n_0 e^{-Z_+ \frac{eY}{k_b T}}, \quad n_- = n_0 e^{-Z_- \frac{eY}{k_b T}} \quad (3)$$

where k_b is the Boltzmann constant, T is the absolute temperature, and n_0 is the bulk ionic number concentration of the electrolyte. The total local charge density, \mathbf{r}_e for a symmetric electrolyte (i.e. the co-ions and counter-ions have the same charge valence, $|Z_+| = |Z_-| = Z_0$), is given by:

$$\mathbf{r}_e = -2eZ_0 n_0 \sinh\left(\frac{Z_0 eY}{k_b T}\right) \quad (4)$$

Combining Eqs. (1) and (4), we can obtain the Poisson-Boltzmann equation:

$$\frac{\partial}{\partial z} \left(\mathbf{e}_r \frac{\partial Y}{\partial z} \right) + \frac{1}{r} \frac{\partial}{\partial r} \left(r \mathbf{e}_r \frac{\partial Y}{\partial r} \right) = \frac{2eZ_0 n_0}{\mathbf{e}_o} \sinh\left(\frac{Z_0 eY}{k_b T}\right) \quad (5)$$

However, in the presence of hydrodynamic flow, the n_+ and n_- ionic number concentration distributions are described by the more general Nernst-Planck equations [23]:

$$\begin{aligned} \frac{\partial n_+}{\partial t} + \frac{\partial(un_+)}{\partial z} + \frac{1}{r} \frac{\partial(vn_+)}{\partial r} &= \frac{\partial}{\partial z} \left(D_+ \frac{\partial n_+}{\partial z} \right) + \frac{1}{r} \frac{\partial}{\partial r} \left(r D_+ \frac{\partial n_+}{\partial r} \right) \\ + \frac{\partial}{\partial z} \left(Z_+ n_+ \frac{eD_+}{k_b T} \frac{\partial Y}{\partial z} \right) + \frac{1}{r} \frac{\partial}{\partial r} \left(r Z_+ n_+ \frac{eD_+}{k_b T} \frac{\partial Y}{\partial r} \right) \end{aligned} \quad (6)$$

$$\begin{aligned} \frac{\partial n_-}{\partial t} + \frac{\partial(un_-)}{\partial z} + \frac{1}{r} \frac{\partial(vn_-)}{\partial r} &= \frac{\partial}{\partial z} \left(D_- \frac{\partial n_-}{\partial z} \right) + \frac{1}{r} \frac{\partial}{\partial r} \left(r D_- \frac{\partial n_-}{\partial r} \right) \\ + \frac{\partial}{\partial z} \left(Z_- n_- \frac{eD_-}{k_b T} \frac{\partial Y}{\partial z} \right) + \frac{1}{r} \frac{\partial}{\partial r} \left(r Z_- n_- \frac{eD_-}{k_b T} \frac{\partial Y}{\partial r} \right) \end{aligned} \quad (7)$$

where D_+ and D_- are the diffusion coefficients of the n_+ and n_- , respectively. u and v are the velocities in the axial and radial direction respectively.

b) Hydrodynamic Field

The axial electric field will induce a body force and the modified Navier-Stokes equation becomes
Continuity equation:

$$\frac{\partial \mathbf{r}}{\partial t} + \frac{\partial(\mathbf{r}u)}{\partial z} + \frac{1}{r} \frac{\partial(r\mathbf{r}v)}{\partial r} = 0 \quad (8)$$

Modified Navier-Stokes equation:

$$\begin{aligned} \frac{\partial(\mathbf{r}u)}{\partial t} + \frac{\partial(\mathbf{r}uu)}{\partial z} + \frac{\partial(\mathbf{r}vu)}{\partial r} &= \frac{\partial}{\partial z} \left(\mathbf{h} \frac{\partial u}{\partial z} \right) \\ + \frac{1}{r} \frac{\partial}{\partial r} \left(\mathbf{h} r \frac{\partial u}{\partial r} \right) - \frac{\partial p}{\partial z} + \mathbf{r}_e \left(E - \frac{\partial Y}{\partial z} \right) \end{aligned} \quad (9)$$

$$\begin{aligned} \frac{\partial(\mathbf{r}v)}{\partial t} + \frac{\partial(\mathbf{r}uv)}{\partial z} + \frac{\partial(\mathbf{r}vv)}{\partial r} &= \frac{\partial}{\partial z} \left(\mathbf{h} \frac{\partial v}{\partial z} \right) \\ + \frac{1}{r} \frac{\partial}{\partial r} \left(\mathbf{h} r \frac{\partial v}{\partial r} \right) - \frac{\partial p}{\partial r} + \mathbf{r}_e \frac{\partial Y}{\partial z} \end{aligned} \quad (10)$$

where \mathbf{r} and \mathbf{h} are the density and viscosity of the fluid respectively, p is the hydraulic pressure. In equation (9), E is the electrical field strength which is yet to be obtained. The electrical field strength for each section will be different and can be determined by

$$E_i = \frac{IR_i}{L_i} \quad (11)$$

where L_i is the length of the i th section, I is the electrical current. R_i is the electrical resistance of the i th section of the electrolyte solution, given as

$$R_i = \frac{L_i}{C_i I_i A} \quad (12)$$

where C_i is the concentration of the i th section, A is the cross-sectional area of the cylindrical capillary and I_i is the molar conductivity of the i th section and is given as:

$$I = I_+ n_+ + I_- n_- \quad (13)$$

where I_+ and I_- are the electric conductivity of cations and anions, respectively. When the total electrical voltage applied to the capillary and electrical resistance are known, the electrical current through the capillary can be determined by:

$$I = \frac{V_t}{R_t} = \frac{V_t}{R_1 + R_2} \quad (14)$$

where V_t is the total electrical voltage applied to the capillary, which is constant during the process. R_t is the total electrical resistance, which is the sum of the resistance of the two sections.

c) Boundary condition

The boundary conditions at the inlet, outlet, wall and at the junction of the step change in zeta potential can be specified as:

Poisson equations:

$$\text{(Inlet)} : \mathbf{y}(r, -L_1) = 0 \quad (15a)$$

$$\text{(Outlet)} : \frac{\partial \mathbf{y}(r, L_2)}{\partial z} = 0 \quad (15b)$$

$$\begin{aligned} \text{(Wall)} : \mathbf{y}(a, z) &= 0, \quad z \leq 0 \\ \mathbf{y}(a, z) &= \mathbf{x}, \quad z > 0 \end{aligned} \quad (15c)$$

$$\text{(Symmetric centerline)} : \frac{\partial \mathbf{y}(0, z)}{\partial r} = 0 \quad (15d)$$

Nernst-Planck equations:

$$\text{(Inlet)} : n_{\pm}(r, -L_1) = n_0 \quad (16a)$$

$$\text{(Outlet)} : \frac{\partial n_{\pm}(r, L_2)}{\partial z} = 0 \quad (16b)$$

$$\text{(Wall)} : n_{\pm}(a, z) = n_0 \exp(-Z_{\pm} \frac{e\mathbf{x}}{k_b T}) \quad (16c)$$

$$\text{(Symmetric centerline)} : \frac{\partial \mathbf{y}(0, z)}{\partial r} = 0 \quad (16d)$$

The pressure boundary conditions are given at both inlet and outlet in the microchannel for solving the momentum equations:

$$\text{(Inlet)} : p(r, -L_1) = p_1, \quad v(r, -L_1) = 0 \quad (17a)$$

$$\text{(Outlet)} : p(r, L_2) = p_2, \quad \frac{\partial u(r, L_2)}{\partial z} = 0 \quad (17b)$$

$$\text{(Wall)} : u(a, z) = v(a, z) = 0 \quad (17c)$$

$$\text{(Symmetric centerline)} : \frac{\partial u(0, z)}{\partial r} = 0, \quad v(0, z) = 0 \quad (17d)$$

where \mathbf{x} is the zeta potential which is a measurable electrical potential at the boundary between the compact and diffuse layer of the EDL, p_1 and p_2 are the pressure at point A and B, respectively.

B. Numerical solution

The coupled electrical field governed by the Poisson-Boltzmann equation (1) and Nernst-Planck equations (6-7), and the hydrodynamics field governed by the modified Navier-Stoke equation (8-10) are solved numerically by finite volume method (FVM). In FVM, the computational domain is discretized by rectangular elements which are named as control volume. The grid point is located at the center of a control volume. The dependent variables, i.e. pressure, are stored at the grid point. The staggered grid system is used for the velocity components. The governing equations integrated over each control volume generating a set of algebraic equations which are solved by using a line-by-line Tri-Diagonal-Matrix Algorithm (TDMA). The combined convection-diffusion effect in the governing equation is modeled by power-law scheme. The pressure-velocity coupling in the momentum equations (9-10) are solved by SIMPLER algorithm [24]. In this study, a numerical solution is considered to have converged as the imbalance of mass flow rate in the continuity equation (8) is less than 10^{-6} .

C. Analytical solution for electroosmotic flow with a step change in zeta potential

Taking a similar approach of Herr et. al. [18], the pressures at points A and B in the region of the zero zeta potential and non-zero zeta potential respectively, depicted in Fig. 1, can be obtained by assuming that fluid flow outside of the junction region (i.e. outside of $-L_1 < z \leq L_2$) is steady, fully developed and with a thin charged double-layer. It can be described by:

$$p_1 = p_{in} + \frac{8E\mathbf{e}_r l_1 l_2 \mathbf{x}}{a^2 (l_1 + l_2)} \quad (18)$$

$$p_2 = p_{out} - \frac{8E\mathbf{e}_r l_1 l_2 \mathbf{x}}{a^2 (l_1 + l_2)} \quad (19)$$

where p_{in} and p_{out} are the pressures at the inlet and outlet, respectively. Once the pressures at point A (p_1) and B (p_2) are solved analytically, the perturbation of electroosmotic flow at the junction region of a step change in zeta potential shown in Fig. 1 can be solved numerically.

III. RESULTS AND DISCUSSIONS

In this study, NaCl was used as the working fluid of electrolyte solution, and its bulk ionic concentration was

chosen as 10^{-4} M. The temperature of the solution was kept at 293K. The radius and length of the cylindrical capillary are $5\mu\text{m}$ and $80\mu\text{m}$, respectively. The measurable zeta potential near the wall of the channel is 40mV. The pressures at inlet and outlet were assumed to be atmospheric pressure. All other constants, thermal and physical properties employed in the computations are listed in Table 1.

Table 1, Material constants, thermal and physical properties

Variable	Unit	Value
D_+ (Eq. 5)	mol/l	1.334×10^{-9}
D_- (Eq. 6)	mol/l	2.032×10^{-9}
e (Eq. 2)	C	1.602×10^{-19}
k_b (Eq. 3)	J/K	1.381×10^{-23}
ϵ_r (Eq. 1)		80
ϵ_0 (Eq. 1)	C/Vm	8.854×10^{-12}
I_+ (Eq. 13)	$\text{m}^2 \cdot \text{S/mol}$	50.080×10^{-4}
I_- (Eq. 13)	$\text{m}^2 \cdot \text{S/mol}$	76.310×10^{-4}
ρ (Eq. 8)	kg/m^3	998
h (Eq. 9)	$N \cdot \text{s/m}^2$	1.005×10^{-3}

The appropriate dimensionless forms of the variables can be defined as:

$$\text{Dimensionless coordinates: } \bar{z} = \frac{z}{a}, \bar{r} = \frac{r}{a} \quad (20a)$$

$$\text{Dimensionless electrical potential: } \bar{\psi} = \frac{Z_0 e \psi}{k_b T} \quad (20b)$$

$$\text{Dimensionless ionic concentration: } \bar{n}_{\pm} = \frac{n_{\pm}}{n_0} \quad (20c)$$

$$\text{Dimensionless velocity: } \bar{u} = \frac{u}{u_{in}}, \bar{v} = \frac{v}{u_{in}} \quad (20d)$$

Dimensionless electrical net charge density:

$$\bar{F}_e = \frac{Z_+ n_+ + Z_- n_-}{Z_0 n_0} \quad (20e)$$

where for a symmetric monovalence electrolyte, $Z_+ = -Z_- = Z_0 = 1$

As shown in Fig. 1, the microchannel has a step change of zeta potential at $z=0$. The non-zero zeta potential region is between $0 \leq z \leq l_2 + L_2$, and the body force is non-zero. In the zero zeta potential region (i.e., $-(l_1 + L_1) \leq z \leq 0$) the

zeta potential is zero and hence the body force is also zero. The electroosmotic flow is fluid flow driven by an applied external electrical potential, and there is no externally applied pressure difference.

Figs. 2(a) and 2(b) show the distributions of the dimensionless electrical potential (Eq. 20(b)) and net charge density (Eq. 20(e)) in the microchannel. It can be observed that both the electrical potential and the net charge density obtained from Boltzmann distributions vary in the non-zero zeta potential region and its EDL reaches a constant thickness in accordance to the implicit assumption of a Boltzmann distribution for an equilibrium charge distribution.

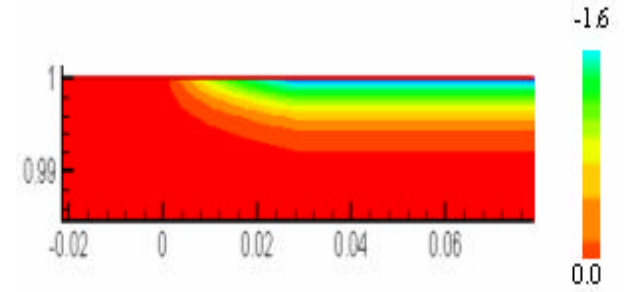


Fig. 2(a) Distribution of dimensionless electrical potential ($\bar{\psi}$) in microchannel with step change of zeta potential.

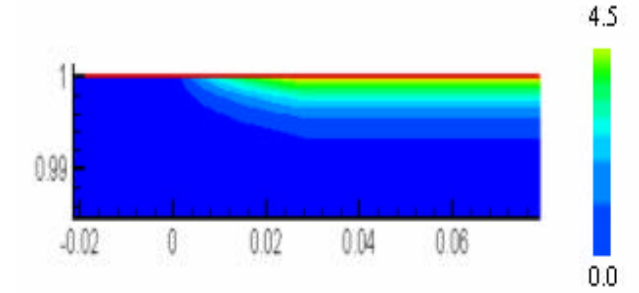


Fig. 2(b) Distribution of dimensionless charge density (\bar{F}_e) in microchannel with step change of zeta potential.

Fig. 3 shows the distributions of both the co-ions and counter-ions (Eq. 20(c)) at two different locations in the non-zero zeta potential region. The EDL development can also be reflected from this cross-sectional distribution of co-ions and counter-ions. Large portion of the channel is occupied by ion concentrations which are the same as the bulk concentration. There is an abrupt change in the ion concentrations near the channel wall due to the existence of zeta potential. As the flow proceeds, there is little variation of ion concentration as $z \geq 0.1$.

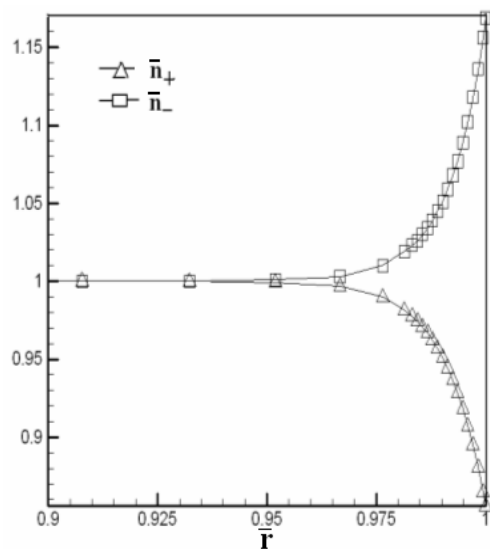


Fig. 3(a) Distribution of concentration of co-ions (\bar{n}_+) and counter-ions (\bar{n}_-) at $\bar{z}=0.1$

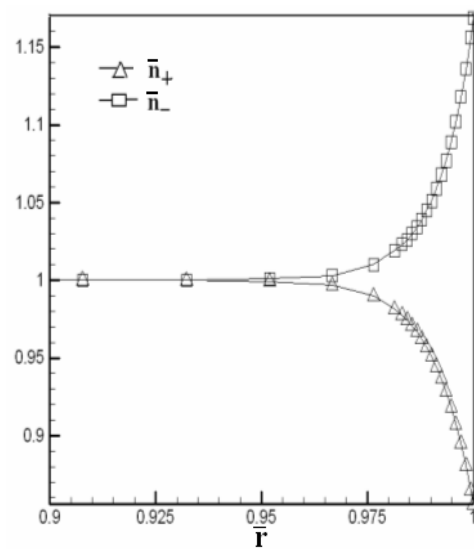


Fig. 3(b) Distribution of concentration of co-ions (\bar{n}_+) and counter-ions (\bar{n}_-) at $\bar{z}>0.1$.

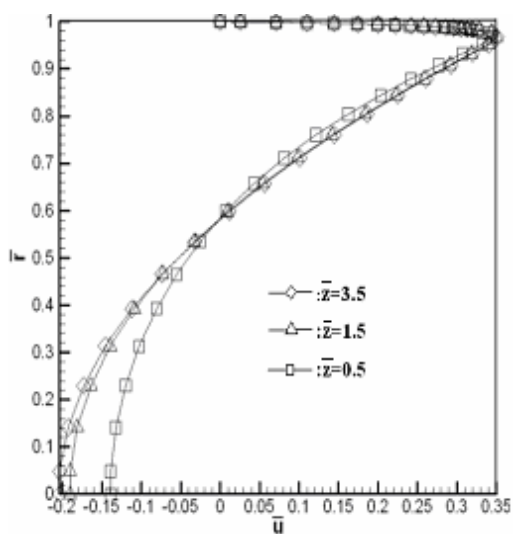


Fig. 4(a) Distribution of dimensionless velocity in non-zero zeta potential region of the microchannel.

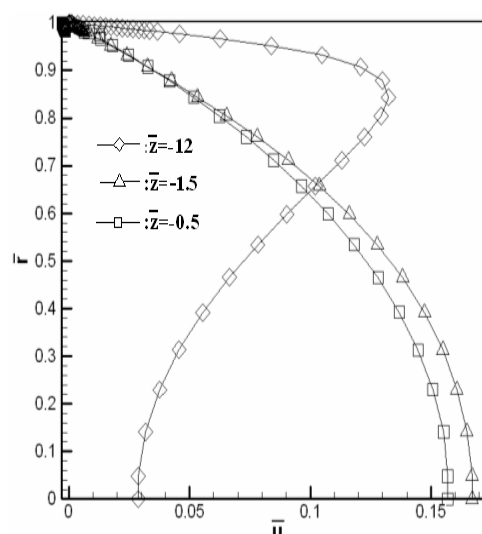


Fig. 4(b) Distribution of dimensionless velocity in the zero zeta potential region of the microchannel.

Fig. 4 shows the evolution of the predicted velocity profiles at different positions along the flow direction in the microchannel. In the non-zero zeta potential region, the flow motion is driven by a body force produced by an externally applied electrical field which acts on the net fluid charge near the wall. The velocity distribution of the fluid motion near the wall is shown in Fig. 4 (a). The velocity is low near the center at the exit of the channel due to the

small driving force there. With the length of non-zero zeta potential region increases, the viscous drag effect increases. This produces higher velocity near the center of the channel. In the zero zeta potential region, the flow motion is driven by a suction effect produced by a flow motion in the non-zero zeta potential region due to charge density distribution. This produces a parabolic velocity profile, see Fig. 4(b).

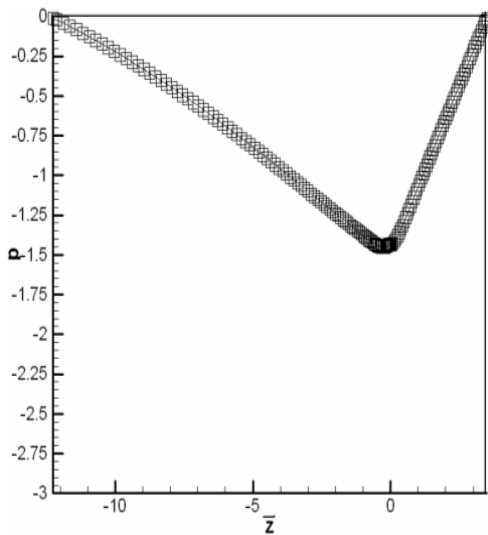


Fig. 5 Induced pressure field distribution along the center-line of microchannel.

Fig.5 shows the induced pressure field distribution along the center-line of the microchannel with a step change in zeta potential. It is observed that a negative pressure gradient exists in the region with zero zeta potential but positive pressure gradient in the region with non-zero zeta potential. Fig.5 shows that pressure decreases from the entrance to a minimum pressure at the junction of the step change in zeta potential at $z=0$. The velocity near the wall increases as shown in Fig. 4(a). In the region with non-zero zeta potential, the positive pressure gradient reduces the velocity, as shown in Fig. 4(b). As such, the requirement of constant flow rate for mass continuity is satisfied.

Fig. 6 shows the pressure distribution along the radial direction at both sides of the junction with a step change in zeta potential. Fig. 6(a) indicates that a non-uniform cross-sectional pressure distribution exists at $z=0.1$. The pressure is positive near the wall, which provides the driving force for fluid flow. Negative non-uniform pressure distribution is observed at $z=-0.1$, which is in the region with zero zeta potential and is driven by the drag force from the EDL of the downstream fluid in the non-zero zeta potential region.

IV. CONCLUSIONS

This study investigated numerically the effects of a step change in zeta potential in a microchannel on electroosmotic flow. A negative pressure gradient is generated in the region with zero zeta potential, which increases the velocity. The velocity profile is parabolic, which is similar to a pressure-driven flow. Conversely, a positive pressure gradient exists in the region with non-zero zeta potential, which decreases the velocity and leads to a distorted velocity profile.

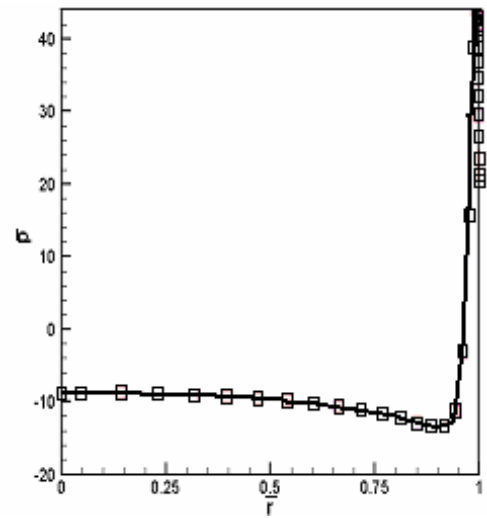


Fig. 6(a) Pressure distribution at $\bar{z}=0.1$ along the radial direction in microchannel.

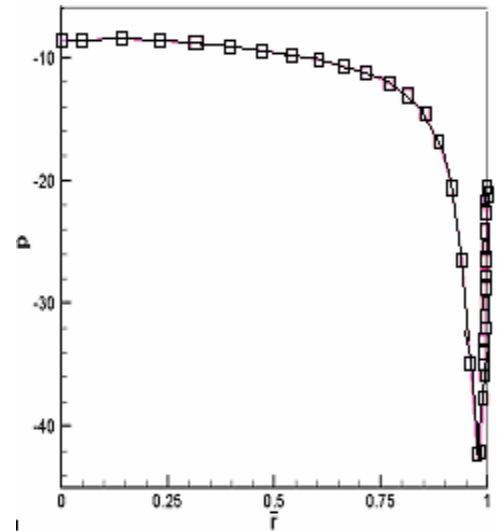


Fig. 6(b) The pressure distribution at $\bar{z}=-0.1$ for the cases along the radial direction in the microchannel.

REFERENCES

- [1] Darwin R ,Dimitri I, Pierre A. and Andreas M, “ Micro Total Analysis Systems. 1. Introduction, Theory, and Technology” , Ana. Chem. ,v74 ,pp2623-2636, 2002.
- [2] Pierre A., Dimitri I, Darwin R and Andreas M, “ Micro Total Analysis Systems. 2. Analytical standard operations and applications” , Ana. Chem. v74,pp2637-2652, 2002.
- [3] Chiu D.T., N.L. Jeon, S. Huang, R.S. Kane, C.J. Wargo, I.S. Choi, D.E. Ingber, and G.M. Whitesides, “ Patterned deposition of cells and proteins onto surfaces by using three-dimensional microfluidic systems” . Proc. Natl. Acad. Sci. USA, v97, pp2408-2413,2000.

- [4] Li J., J.F. Kelly, I. Chernushevich, D.J. Harrison and P. Thibault, "Separation and identification of peptides from gel-isolated membrane proteins using microfabricated device for combined capillary electrophoresis /nanoelectrospray mass spectrometry". *Anal. Chem.* v72, pp 599-609,2000.
- [5] Brody J. P., A.E. Kamholz, and P. Yager, "Prominent microscopic effects in microfabricated fluidic analysis systems, *Proc. Micro. Nano-fabricated Electro-opt.*" *Mech. Systems Biomed. Environ. Appl.* , pp103-110, 1997
- [6] Chan J.H., A.T. Timperman, D.Qin and R. Aebersold, "Microfabricated polymer devices for automated sample delivery of peptides for analysis by electrospray ionization tandem mass spectrometry", *Anal. Chem.* v71,pp4437-4444, 1999.
- [7] Jacobson SC, McKnight TE and Ramsey JM, "Microfluidic devices for high-efficiency separations", *Anal. Chem.*,v71, pp4455-4459,1999.
- [8] Jeon NL, Dertinger KW, Chiu DT, Choi IS, Stroock AD and Whitesides GM, "Generation of solution and surface gradients using microfluidic systems", *Langmuir*, v16, pp8311-8316,2000.
- [9] Probstein RF, "Physicochemical hydrodynamics: an introduction", New York: Wiley-Interscience ,1994.
- [10] Kamholz A., B. Weigl, B. Finlason and P. Yager, "Quantitative analysis of molecular interaction in a microfluidic channel: the T-sensor", *Anal. Chem.*, v71, pp5340-47,1999.
- [11] Yang C., and Li DQ., "Electrokinetic effects on pressure-driven liquid flows in rectangular microchannels", *J. Colloids Interface Sci.*, 194, 95-107,1997
- [12] Yang C., Li DQ. and Masliyah, JH, "Modeling forced liquid convection in rectangular microchannels with electrokinetic effects", *Int. J. of Heat Mass Transfer*, 41, 4229-4249(1998)
- [13] Patankar, NA and Hu HH, "Numerical simulation of electroosmotic flow", *Anal. Chem.* 70, 1870-1881,1998
- [14] Anderson, JL and Idol WK, "Electroosmosis through pores with nonuniformly charged walls", *Chem. Eng. Commun.* 38,93-106 ,1985
- [15] Potocek B, Gas, B, Kenndler, E and Stedry M, "Electroosmosis in capillary zone electrophoresis with nonuniform zeta-potential", *J. Chromatogr. A*, 709, 51-62,1995
- [16] Long, D Stone HA and Ajdari A,"Electroosmotic flows created by surface defects in capillary electrophoresis", *J. Colloid Interface Sci.*, 212: 338-349 ,1999
- [17] Stroock, AD, Weck M, Chiu DT, Huck WTS, Knnis PGA, Ismagilov RF and Whitesides, GM," Patterning electro-osmotic flow with patterned surface charge", *Phys. Rev. Lett*, 84:3314-3317, 2000
- [18] Herr, AE, Molho, JI, Santiago JG, Mungal, MG and Kenny, TW, "Electroosmotic capillary flow with nonuniform zeta potential", *Anal. Chem.*, 72: 1053-1057, 2000
- [19] Ren L, Qu W and Li DQ, " Interfacial electrokinetic effects on liquid flow in microchannels", *Int. J. Heat Mass Transfer*, 44:3125-,2001
- [20] Ren L and Li DQ," Electroosmotic flow in heterogeneous microchannels", *J. Colloid Interface Sci.*, 243:255-261,2001
- [21] Yang RJ, Fu LM and Lin YC," Electroosmotic flow in microchannels", *J. Colloid Interface Sci.* 236:98-105, 2001
- [22] Fu LM, Lin JY and Yang RJ," Analysis of electroosmotic flow with step change in zeta potential", *J. Colloid Interface Sci.* 258: 266-275, 2003
- [23] Masliyah, *Electrokinetic Transport Phenomena*, AO STRA technical publication series No.12, AO STRA, Edmonton, 1994
- [24] Patankar SV, *Numerical Heat Transfer and Fluid Flow*, Hemisphere, New York, 1980.